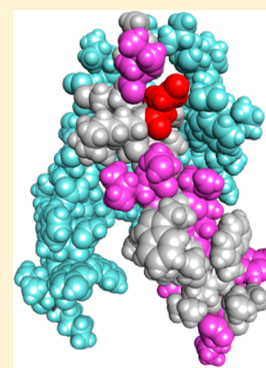


The Membrane Proximal External Regions of gp41 from HIV-1 Strains HXB2 and JRFL Have Different Sensitivities to Alanine Mutation

Hyun Ah Yi, Barbara Diaz-Rohrer, Priyanka Saminathan, and Amy Jacobs*

Department of Microbiology and Immunology, School of Medicine and Biomedical Sciences, University at Buffalo, The State University of New York, Buffalo, New York 14214, United States

ABSTRACT: The transmembrane subunit (gp41) of the HIV envelope protein complex (Env) mediates the viral fusion step of HIV entry. The membrane proximal external region (MPER), one of the functional domains of gp41, has been the focus of a great deal of research because it is a target for neutralizing antibodies. In this study, we examined 23 amino acid residues in the MPER (660–683) in both a CXCR4 coreceptor-utilizing strain (HXB2) and a CCR5-utilizing strain (JRFL) by alanine scanning mutagenesis. Despite the high degree of gp41 sequence conservation, the effects of alanine mutation in the MPER were different between the two strains. Most mutations in HXB2 had fusogenicity and protein expression levels not less than 50% of that of the wild type in the case of cell–cell fusion. However, ~30% of the mutants in HXB2 showed a severe defect in fusogenicity in viral entry. Mutations in the MPER of strain JRFL had more dramatic effects than that in HXB2 in cell–cell fusion and viral entry. The fact that there are large differences in the effects of mutation between two strains suggests the potential for the interaction of the MPER with nonconserved sequences such as the fusion peptide and/or other NHR domains as well as potential long-range structural effects on the conformational changes that occur with the Env complex during membrane fusion.



The HIV-1 envelope protein (Env) is expressed as a precursor protein (gp160) and cleaved by a cellular protease into two subunits: the surface subunit (gp120) and the transmembrane subunit (gp41). The transmembrane subunit (gp41) mediates membrane fusion and is composed of several domains: the fusion peptide, the N-terminal heptad repeat (NHR), the loop region, the C-terminal heptad repeat (CHR), followed by the membrane proximal external region (MPER), and the transmembrane region (Figure 1).¹

The MPER is located proximal to the viral lipid bilayer at the C-terminal end of the ectodomain portion of gp41. The MPER is highly conserved and is essential for membrane fusion.² A conserved tryptophan-rich motif plays an important role in Env-mediated fusion and infectivity.³ Five tryptophan residues in the MPER are known to be involved in fusion pore expansion.⁴

The MPER has been one of the important targets in HIV vaccine development.^{5–7} Human antibodies 2F5, 4E10, Z13el, and 10E8 bind to the MPER and neutralize a broad range of HIV-1 strains.^{8–14} These broadly neutralizing antibodies are known to disrupt MPER function and membrane fusion.^{15,16} The MPER sequence also makes up a portion of the only peptide entry inhibitor in the clinic, T20 (brand name, Fuzeon; generic name, enfuvirtide) as it contains 14 of the MPER amino acid residues.^{17–19} The MPER is an important region to manipulate in attempts to improve immunogenicity and elicit neutralizing antibodies.^{20–25}

There are issues, however, with utilizing the MPER as a target. The MPER is occluded by steric hindrance caused by quaternary Env packing and is exposed only transiently at a relatively late stage in the entry mechanism.^{26–29} Inaccessibility to the MPER due to the viral membrane and structure of the

Env trimer remains one of the obstacles in developing vaccines and therapeutic intervention methods targeted to this region.⁵

There are several crystal structures of HIV gp41, but most atomic level structures contain only the gp41 core consisting of the two helical heptad repeats and the middle loop region.^{30–33} The structure of full length intact gp41 with the MPER and the transmembrane region has not been determined at the atomic level. There have been recent reports of smaller gp41 constructs that include the MPER sequence. One reported X-ray crystallographic structure consists of CHR and MPER constructs (residues 630–680) that form an asymmetric dimer with itself.³⁴ Another structural study included the NHR, CHR, and MPER and suggests that the MPER portion is a long, slightly bent helix and relatively flexible.³⁵ There is a report of a crystal structure of gp41 (residues 528–680) including the MPER and the fusion peptide that is located upstream of the NHR.³⁶ This report suggests that the structure has an ~90° turn of the MPER at N677.

As gp41 is a membrane protein and the viral membrane is involved in neutralization by neutralizing antibodies, it is important to consider this region in the context of the lipid environment.³⁷ The structure of the MPER in the lipid environment is not clearly understood, but there are diverse structures that have been proposed. One study suggests a metastable L-shaped structure embedded on a membrane surface.¹⁶ The L-shaped MPER structure consists of a helix and a flexible hinge followed by another helix. This L-shaped MPER structure can be disrupted by neutralizing antibodies.¹⁵ Another

Received: September 17, 2014

Revised: January 28, 2015

Published: February 3, 2015



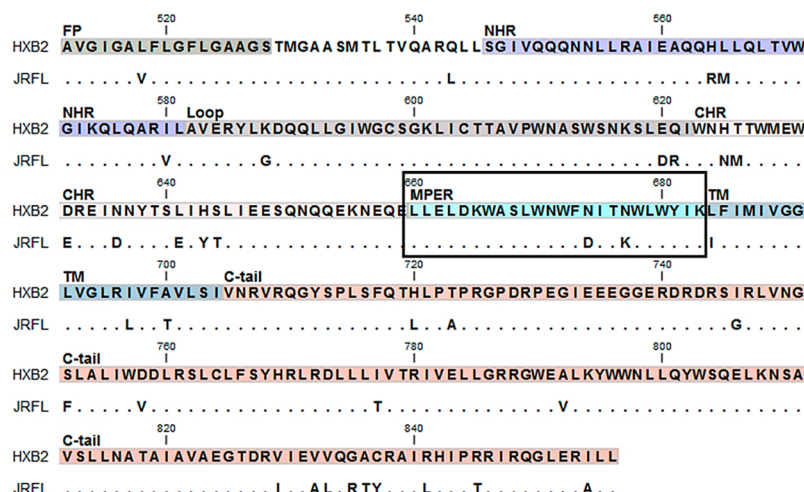


Figure 1. Alignment of the gp41 amino acid sequence highlighting the MPER from HXB2 and the JRFL strains. gp41 begins at the N-terminus with the fusion peptide (FP) followed by the N-terminal heptad repeat (NHR), a loop, the C-terminal heptad repeat (CHR), a membrane proximal external region (MPER), and a transmembrane domain (TM) followed by a C-terminal cytoplasmic region (C-tail). The gp41 amino acid sequence was aligned using CLC Main Workbench 7.5.1. The numbering is based on that of the HXB2 strain, and matching residues are shown as dots. The boxed area indicates the MPER region. We introduced 23 alanine substitutions into both strain HXB2 and strain JRFL.

structural study of the trimeric MPER on a detergent micelle shows a symmetrical α -helical conformation with a bend between the 2F5 and 4E10 epitopes.³⁸ A recent study shows that the MPER can have at least two stable conformations in the lipid bilayer, suggesting that the topology can be switched depending upon the physiological environment.³⁹ Taken together, evidence suggests that flexibility in the MPER may be partially responsible for poor immunogenicity.

With this report, the study of gp41 by alanine scanning mutagenesis in the literature encompasses the NHR, CHR, loop region, and now the MPER, providing insights into the role and importance of each residue in the gp41 ectodomain.^{40–42} Herein, we report alanine scanning studies of the MPER using both CXCR4 and CCR5 utilizing strains to determine the importance of each amino acid in cell–cell fusion and viral entry. These studies help to identify critical regions for potential intervention and also regions that have the potential to be subjected to manipulations for labeling for ultrastructural studies without detrimental effects on function. This is especially important for domains such as the MPER that are critical in the membrane fusion process.

EXPERIMENTAL PROCEDURES

Plasmids and Mutagenesis. The envelope protein-expressing plasmids that contain alanine mutations on the MPER were prepared as described previously⁴¹ from pHXB2-env⁴³ and pJRFL-env⁴⁴ using the QuikChange II XL site-directed mutagenesis kit (Stratagene) and were verified by DNA sequencing (Roswell Park Cancer Institute DNA Sequencing Laboratory). The plasmid-expressing HIV Rev protein, pRev-1,⁴⁵ and the plasmid-expressing Tat protein, pCEP4-Tat,⁴⁶ were used in the cell–cell fusion assay. The HIV backbone plasmid, pNL4-3.HSA.R-E,⁴⁷ was used in the production of HIV pseudovirus.

Cell Culture. TZM-bl⁴⁸ and 293T (ATCC) cells were maintained in Dulbecco's modified Eagle's medium (DMEM) that contained 10% fetal bovine serum (FBS) and 1% penicillin-streptomycin. Cells were incubated in a 5% CO₂ incubator with humidification at 37 °C.

Cell–Cell Fusion Assay. For the cell–cell fusion assay, the wild type (WT) or alanine mutants of the envelope plasmid, pHXB2-env or pJRFL-env, were transfected with pRev⁴⁵ and pTat⁴⁶ plasmids by a standard polyethylenimine transfection⁴⁹ into 293T cells; 5×10^5 293T cells per well were prepared the day before the transfection, and 3 μ g of envelope plasmid and 0.8 μ g of each pRev and pTat plasmid were used per well for the transfection in a six-well plate. At 24 h post-transfection, the cells were detached from the plate and seeded at a density of 5×10^4 cells/well along with 5×10^4 cells/well of TZM-bl in a 96-well plate. The plate was incubated for an additional 24 h at 37 °C in a 5% CO₂ incubator, and membrane fusion activity was measured by a luciferase assay (One-glo, Promega) according to the manufacturer's protocol. Fusion levels were normalized to the fusion level of WT envelope protein-expressing cells.

Virus Entry Assay. HIV-1 was produced by cotransfection of 10 μ g of plasmids encoding envelope protein, either WT or mutant, and 10 μ g of pNL4-3.HSA.R-E⁴⁷ into 293T cells in a 100 mm dish as described previously.⁵⁰ The HIV-1 p24 antigen capture enzyme-linked immunoassay (AIDS & Cancer Virus Program, National Cancer Institute at Frederick, Frederick, MD) was performed to determine the p24 concentration of mutant enveloped viral particles as well as WT virus.

TZM-bl cells were seeded at a density of 2×10^4 cells/well in a 96-well plate, and virus was added at the equivalent of 100 ng of p24 per well. The virus was spinoculated at 1000g for 1 h at room temperature and then incubated at 37 °C in a 5% CO₂ incubator.^{50,51} At 48 h postinfection, viral entry levels were measured by a luciferase assay as described above.

Western Blot Analysis. Cellular pellets were lysed using M-PER mammalian protein extraction reagent (Thermo Scientific) containing protease inhibitor cocktail (Roche). The virus pellet was prepared by ultracentrifugation at 55000 rpm for 1 h using a Beckman SW55Ti rotor. The pellets were resuspended in lysis buffer [50 mM Tris (pH 7.5), 150 mM NaCl, 5 mM EDTA, 0.5% Nonidet P-40, and 0.1% SDS].^{40,41}

Protein was quantified using a BCA protein assay (Pierce), and sodium dodecyl sulfate–polyacrylamide gel electrophoresis

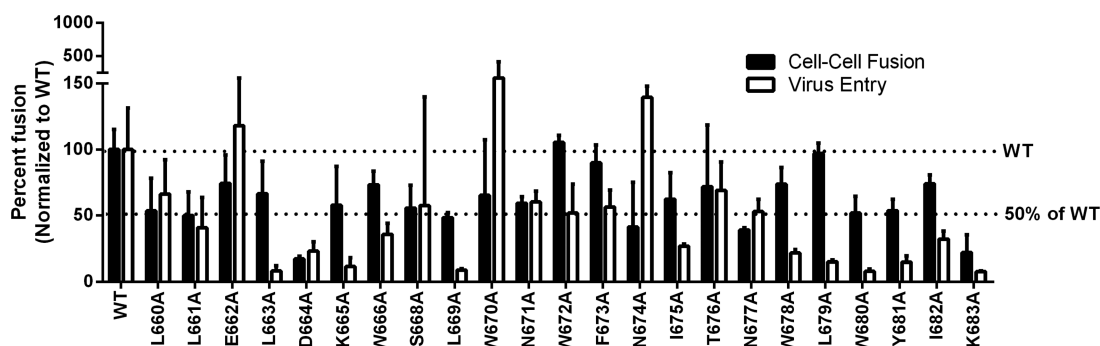


Figure 2. Effects of alanine substitution on HXB2 Env-mediated cell–cell fusion and viral entry. For cell–cell fusion (black bars), each mutant plasmid was transfected into 293T cells along with plasmids expressing the tat and rev proteins. The transfected cells were then co-incubated with receptor cell line TZM-bl for 24 h. Fusion activity was measured by a luciferase assay. For viral entry (white bars), each mutant was transfected into 293T cells along with the HIV backbone plasmid and virus was harvested after 48 h. The amount of virus was determined by a p24 antigen capture enzyme-linked immunosorbent assay, and virus stocks with an equivalent amount of p24 protein (100 ng) were added to each well of TZM-bl cells. Viral entry levels were determined by a luciferase assay 48 h post infection. The WT level and the 50% level of WT fusion are indicated with dotted lines.

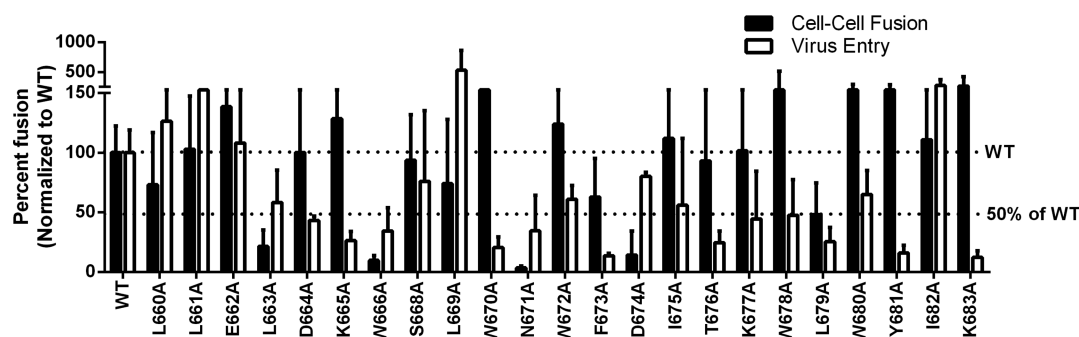


Figure 3. Effects of alanine substitution on JRFL Env-mediated cell–cell fusion and viral entry. Cell–cell fusion (black bars) and viral entry levels (white bars) were measured as described in the legend of Figure 2 using JRFL Env mutants.

(SDS–PAGE) was performed. After the transfer, the nitrocellulose membranes were blocked with the blocking buffer (LI-COR) and then simultaneously probed with the mouse anti-HIV-1 gp41 monoclonal antibody (Chessie-8⁵²) and the goat anti-HIV-1 gp120 polyclonal antibody (USBiological).

The secondary antibodies used in this study were IR800-conjugated donkey anti-mouse IgG (LI-COR) for gp41 and IR680-conjugated rabbit anti-goat IgG (LI-COR) for gp120. For the quantification, p24 levels were also analyzed by reprobing the membrane with the anti-HIV-1 p24 monoclonal antibody.⁵³

The membranes were scanned by the Odyssey Infrared Imaging System (LI-COR). Data for the quantification of each band were obtained from the integrated intensities (II) after the median background subtraction method. The II from each band was used to calculate the relative expression levels of proteins. For virus and virus-producing cells, the relative expression was calculated as follows: $\{[(\text{II of mutant Env})/(\text{II of p24})]/[(\text{II of WT Env})/(\text{II of p24})]\} \times 100$. In this way, the relative expression ratio of gp41, gp120, and gp160 from each mutant was obtained. For the transfected cells used for the cell–cell fusion assay, normalization was to the WT level of gp41, gp120, and gp160 respectively, as there is no expression of p24 in this case.

RESULTS

Gp41 MPER Alanine Scanning. Two different coreceptor-utilizing HIV strains were used in this study: HXB2 for CXCR4

usage and JRFL for CCR5 usage. We compared the entire amino acid sequence of gp41 from both HXB2 (NCBI GenBank accession number K03455.1) and JRFL (NCBI GenBank accession number U63632.1). There was ~96% identity (821 of 856) in the gp41 amino acid sequence between HXB2 and JRFL, indicating a high degree of conservation in the gp41 sequence between these two strains (Figure 1).

The MPER domain is defined as a total of 24 amino acid residues (660–683 in the HXB2 envelope sequence) based on structural studies and the HIV genome (Figure 1, boxed area). Between HXB2 and JRFL, only two residues are different (22 of 24 residues identical). One is residue 675, and the other is residue 678. Overall, there is 92% amino acid sequence identity between these two strains in the MPER (Figure 1, boxed area). A total of 23 amino acids of 24 were substituted with alanine as residue 667 is already an alanine.

Cell–Cell Fusion and Viral Entry of gp41 MPER Mutants. To determine the effects of alanine mutagenesis on the MPER, a cell–cell fusion and a viral entry assay were performed as described previously.⁴¹ For both cases, we performed three sets of experiments and obtained the average of the fusion levels, and then the fusion levels of each alanine mutant were compared to WT levels.

Figures 2 and 3 show activity in cell–cell fusion and viral entry in the HXB2 strain and the JRFL strain, respectively. Tables 1 and 2 give a summary of these data.

For cell–cell fusion, levels of most HXB2 alanine-substituted mutants were not <50% of that of WT with the exception of

Table 1. Effect of Alanine Mutations on HXB2 Envelope Protein

	cell–cell fusion				virus entry			
	gp120 level ^a	gp41 level ^b	fusion category ^c	effect of alanine mutation ^f	gp120 level ^c	gp41 level ^d	fusion category ^e	effect of alanine mutation ^f
L660A	+++++	+++++	WT	–	++++	++++	WT	–
L661A	+++++	++++	diminished	–	++++	+++	diminished	–
E662A	+++++	++++	WT	–	++++	+++++	WT	–
L663A	++++	+++	WT	–	++++	++++	abolished	severe defect
D664A	++++	++++	abolished	severe defect	++++	++++	diminished	–
K665A	++++	++++	WT	–	++++	++++	abolished	severe defect
W666A	+++++	+++++	WT	–	++++	+++	diminished	–
S668A	+++++	++++	diminished	–	++++	++++	WT	–
L669A	+++	++++	diminished	mild defect	+++	+++	abolished	severe defect
W670A	++++	++++	WT	–	++++	++++	enhanced	increased Env expression
N671A	++++	+++++	diminished	–	++++	+++++	diminished	–
W672A	+++++	+++++	WT	–	++++	++++	WT	–
F673A	+++++	+++++	WT	–	++++	++++	diminished	–
N674A	+++++	++++	diminished	–	++++	++++	enhanced	enhanced fusogenicity
I675A	++++	++++	WT	–	++++	++++	diminished	–
T676A	+++++	+++++	WT	–	+++++	++++	diminished	–
N677A	++++	+++++	diminished	–	++++	++++	diminished	–
W678A	+++++	+++++	WT	–	++++	++++	diminished	–
L679A	+++++	+++++	WT	–	++++	++++	abolished	severe defect
W680A	+++++	+++++	diminished	–	+	+++	abolished	association
Y681A	++++	+++++	diminished	–	++++	+++	abolished	severe defect
I682A	+++++	+++++	WT	–	++++	++++	diminished	–
K683A	++++	+++++	diminished	–	++++	+++	abolished	severe defect

^agp120 protein levels in the cell lysates used for cell–cell fusion. ^bgp41 protein levels in the cell lysates used for cell–cell fusion. ^cgp120 protein levels of expression shown in virus. The levels of protein expression are as follows: +, 0–20% of WT levels; ++, 20–50% of WT levels; +++, 50–80% of WT levels; ++++, >80% of WT levels; +++++, >120% of WT levels. ^dgp41 protein levels of expression shown in virus. The levels of protein expression are as follows: +, 0–20% of WT levels; ++, 20–50% of WT levels; +++, 50–80% of WT levels; ++++, >80% of WT levels; +++++, >120% of WT levels. ^eFusion categories are defined as follows: WT, no effect, WT level; diminished, 20–80% of that of the wild type; abolished, <20% of that of the wild type; enhanced, >120% of that of the wild type. ^fEffects of alanine mutations are defined as follows: expression/folding (<20% of that of WT gp41), cleavage (<20% of that of gp120 and gp41, WT level of gp160), association (gp120/gp41 ratio of <0.5), severe fusogenicity (>20% of that of WT gp41, gp120/gp41 ratio of >0.5, <20% of the WT fusion level), mild fusogenicity (>20% of that of WT gp41, gp120/gp41 ratio of >0.5, 20–80% of the WT level), increased level of Env expression (>120% of that of WT gp160 proteins and fusion level), and enhanced fusogenicity (>120% of that of WT fusion, WT gp160 expression level).

D664, for which the fusion level was extremely low (Figure 2, black bars, and Table 1, left portion). These data indicate that there were only modest effects if any on cell–cell fusion caused by alanine mutation in the MPER of HXB2.

However, levels differed significantly in viral entry (Figure 2, white bars, and Table 1, right portion). Seven mutants (L663A, K665A, L669A, L679A, W680A, Y681A, and K683A) showed abolished fusion activity in viral entry. Five mutants had <50% activity (D664A, W666A, I675A, W678A, and I682A). Two mutants, W670A and N674A, had enhanced fusion levels in viral entry. The levels of the remaining mutations were either WT level or moderately diminished. In general, alanine substitution in the HXB2 MPER was more deleterious in viral entry than in cell–cell fusion.

The alanine-substituted mutants of JRFL were more variable in cell–cell fusion than were mutations in strain HXB2 (Figure 3, black bars, and Table 2, left portion). One mutant, D674A, had diminished cell–cell fusion activity compared to that of WT. There were three mutants (L663A, W666A, and N671A) that exhibited abolished activity in cell–cell fusion. Four other mutants (W678A, W680A, Y681A, and K683A) had an enhanced level of fusion. The levels of the remaining mutations were the same as that of WT in cell–cell fusion.

The viral entry levels in strain JRFL varied dramatically, as well (Figure 3, white bars, and Table 2, right portion). Three mutants (L661A, L669A, and I682A) had increased levels of

viral entry. Many were decreased to below 50% of that of WT (K665A, W670A, F673A, T676A, L679A, Y681A, and K683A). The levels of very few mutations were near the WT level. These included L660A, E662A, and S668A. On a general level, JRFL viral entry was very sensitive to alanine scanning mutations in the MPER.

Mutant Expression, Processing, and gp120–gp41 Association Effects. Alanine mutation of each residue in the MPER could have effects on (1) protein expression or folding of precursor protein gp160 and trafficking of the protein to the plasma membrane via the endoplasmic reticulum and Golgi apparatus, (2) proteolytic cleavage of the precursor gp160 protein to the gp41 and gp120 subunits by the cellular enzyme furin, (3) association between gp41 and gp120, or (4) a defect in fusogenicity.

To determine which of these steps were affected by the mutation, Western blot analysis was performed. The data were quantified and normalized as described in Experimental Procedures. Tables 1 and 2 summarize the effects of alanine mutations in cell–cell fusion and viral entry for HXB2 and JRFL, respectively.

HXB2 MPER Mutant Expression, Processing, and gp120–gp41 Association. Most HXB2 mutants produced cell–cell fusion levels not less than 50% of WT levels. D664 was one of the residues most dramatically affected. Most mutants, including D664A, expressed all Env proteins at WT

Table 2. Effect of Alanine Mutation on JRFL Envelope Protein

	cell–cell fusion				virus entry			
	gp120 expression ^a	gp41 expression ^b	fusion category ^c	effect of alanine mutation ^f	gp120 level ^c	gp41 level ^d	fusion category ^e	effect of alanine mutation ^f
L660A	+++	++++	WT	–	+++++	+++++	WT	–
L661A	+++++	+++++	WT	–	+++++	+++++	WT	–
E662A	+++++	+++++	WT	–	+++++	+++++	WT	–
L663A	+++	+++++	abolished	severe defect	+++++	+++++	WT	–
D664A	+++++	+++++	WT	–	++++	+++++	diminished	–
K665A	+++	+++++	WT	–	+++++	+++++	diminished	mild defect
W666A	+++++	+++++	abolished	severe defect	++++	++	diminished	–
S668A	+++	+++++	WT	–	+++++	+++++	WT	–
L669A	+++++	+++++	WT	–	+++++	+++++	enhanced	increased Env expression
W670A	+++++	+++++	WT	–	+++++	+++++	diminished	mild defect
N671A	+	+++	abolished	–	+	+++++	diminished	expression/association
W672A	++++	+++++	WT	–	++	++++	WT	association
F673A	+++	+++++	WT	–	+++++	++++	diminished	mild defect
D674A	+++++	+++++	diminished	mild defect	++	++	WT	–
I675A	++++	+++++	WT	–	+++++	+++++	WT	–
T676A	++++	+++++	WT	–	+++++	+++++	diminished	mild defect
K677A	+++++	+++++	WT	–	+++++	+++++	WT	–
W678A	++	+++++	enhanced	increased Env expression	+++++	++++	WT	–
L679A	+	+++	WT	–	+++++	+++++	diminished	mild defect
W680A	+	+++	enhanced	enhanced fusogenicity				
	+++++	+++++	WT	–				
Y681A	++	+++	enhanced	enhanced fusogenicity	+++++	++++	diminished	mild defect
I682A	+	+++	WT	–	+++++	+++++	enhanced	increased Env expression
K683A	++++	+++++	enhanced	increased Env expression	++++	++++	diminished	mild defect

^agp120 protein levels in the cell lysates used for cell–cell fusion. ^bgp41 protein levels in the cell lysates used for cell–cell fusion. ^cgp120 protein levels of expression shown in virus. The levels of protein expression are as follows: +, 0–20% of WT levels; ++, 20–50% of WT levels; +++, 50–80% of WT levels; +++++, >80% of WT levels; ++++++, >120% of WT levels. ^dgp41 protein levels of expression shown in virus. The levels of protein expression were shown as follows: +, 0–20% of WT levels; ++, 20–50% of WT levels; +++, 50–80% of WT levels; +++++, >80% of WT levels; ++++++, >120% of WT levels. ^eFusion categories are defined as follows: WT, no effect, WT level; diminished, 20–80% of that of the wild type; abolished, <20% of that of the wild type; enhanced, >120% of that of the wild type. ^fEffects of alanine mutations are defined as follows: expression/folding (<20% of that of WT gp41), cleavage (<20% of that of gp120 and gp41, WT level of gp160), association (gp120/gp41 ratio of <0.5), severe fusogenicity (>20% of that of WT gp41, gp120/gp41 ratio of >0.5, <20% of the WT fusion level), mild fusogenicity (>20% of that of WT gp41, gp120/gp41 ratio of >0.5, 20–80% of the WT level), increased Env expression (>120% of that of WT gp160 proteins and fusion level), and enhanced fusogenicity (>120% of that of WT fusion, WT gp160 expression level).

levels as seen in the cell lysate from the cell–cell fusion experiments (Figure 4A). That of L663A was slightly diminished, but the cell–cell fusion level was not dramatically affected. The protein levels of L669A and W670A were diminished; however, the cell–cell fusion effects were not dramatic. Most mutants had WT levels of cleavage, association, and fusogenicity (Figure 4A and Table 1, left portion). D664A had a fusogenicity defect as the levels of protein expression, cleavage, and association appeared to be near WT levels. Generally, scanning alanine mutations in the MPER of HXB2 did not cause dramatic effects on cell–cell fusion at most residues.

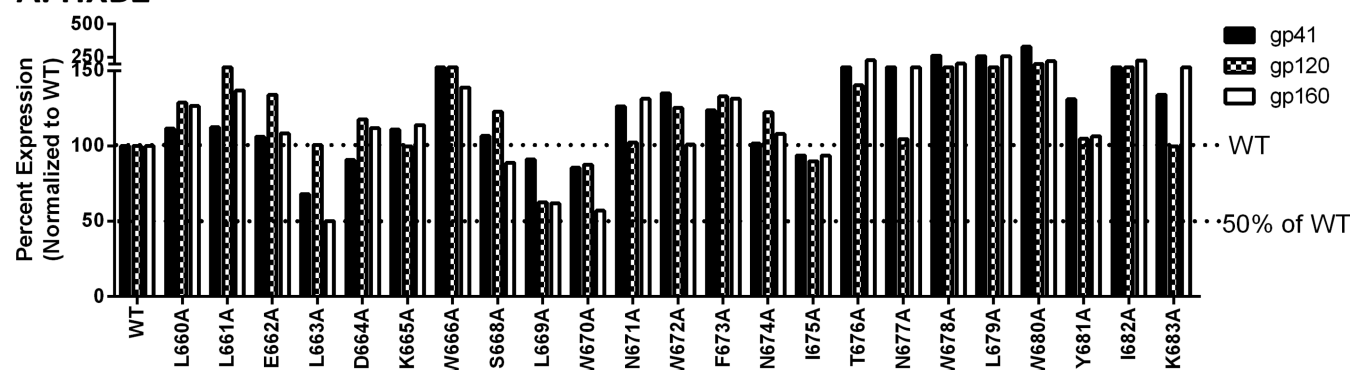
However, the viral entry results are quite different. Most HXB2 mutants had impacts on viral entry from alanine substitution. Six of these mutants (L663A, K665A, L669A, L679A, Y681A, and K683A) showed either a WT or a minimally decreased Env expression level in both the producer cells and the virus samples (Figures 5A and 6B and Table 1, right portion). Some of these mutants (L663A, K665A, and Y681A) also had near normal levels of cleavage and gp41–gp120 association, whereas the level in viral entry was abolished, indicating a defect in fusion. Alanine mutation of these residues had a weaker impact on cell–cell fusion (Figure 2, black bars), suggesting they play a more critical role in viral

entry. L669A had a very small amount of gp120 in the producer cell lysate, but the protein levels on the virus were not decreased below 50%. L679A had a lowered level of gp160 expression along with a lowered level of gp41 in the producer cell lysate; however, the levels on the virus were not dramatically decreased. K683A had a lowered level of expression but WT levels of gp41 and gp120 in the producer cells and levels in the virus not decreased below 50% of that of WT.

One mutant, W680A, had WT levels in the producer cell lysate; however, the level of gp41 on the virus was diminished to approximately 50%, and gp120 was undetectable. This suggests both an incorporation defect due to the lowered level of gp41 on virus and an association defect. The ratio of the levels between gp120 and gp41 was calculated to be <0.5, which implies that there is an association defect. This resulted in a severe disruption of viral entry in the case of W680A.

Finally, two mutants, W670A and N674A, had enhanced levels of viral entry. W670A had a higher level of gp160, gp41, and gp120 in the producer cell lysate. N674A, on the other hand, had increased levels of gp160 and gp41 in the producer cell lysate but a decreased level of gp120. Despite this, both mutations (W670A and N674A) had higher levels of gp120 in

A. HXB2



B. JRFL

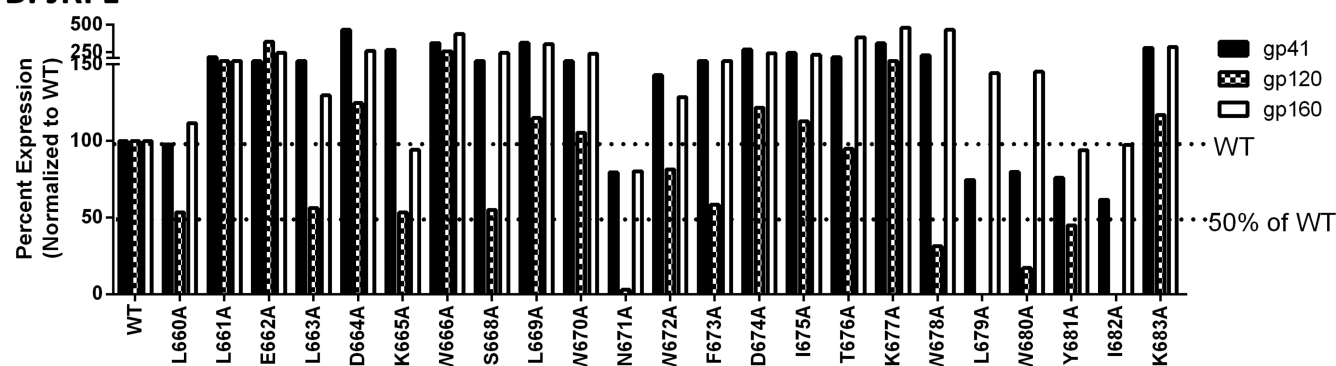


Figure 4. Protein expression level in the cell lysates used for cell–cell fusion. 293T cells transfected with Env-, Tat-, and Rev-expressing plasmids. The cells were lysed, and the total protein concentration was quantified by a BCA assay. An equal amount of protein from each transfected cell sample was loaded onto an SDS–PAGE gel followed by Western blot analysis using Chessie-8 (for gp41 and gp160) and anti-gp120 antibodies. Each membrane was scanned, and the band intensity was quantified. The band intensities of gp41, gp160, and gp120 were normalized to the WT level of each protein: (A) protein expression level of HXB2 Env and (B) protein expression level of JRFL Env.

the virus particles than of gp41, which was closer to the wild-type level.

JRFL MPER Mutant Expression, Processing, and gp120–gp41 Association. In contrast to strain HXB2, alanine mutation of the JRFL strain had far greater effects on cell–cell fusion, and effects were seen in viral entry, as well (Figures 4B–6B and Table 2). Five of the mutants (L660A, K665A, S668A, L679A, and I682A) that produced WT fusion levels in cell–cell fusion had a lower level of gp120 than of gp160 (left portion in Table 2). Nevertheless, this resulted in only a minimal effect on the cell–cell fusion levels that were near the WT level.

Two mutants (L663A and N671A) had abolished levels of cell–cell fusion and also had low levels of gp120 compared to gp160 expression. Another mutant, W666A, which had abolished levels of cell–cell fusion expressed Env protein at the WT level and had wild-type levels of gp41 and gp120. This indicates that the alanine mutation of W666 causes a fusogenicity defect.

There are also mutants (W678A, W680A, Y681A, and K683A) that had increased levels of cell–cell fusion. Interestingly, W678A, W680A, and Y681A all had an increased level of Env protein expression (gp160), a high level of gp41, but a very low level of gp120. Similarly, only K683A had an increased cell–cell fusion level along with increased levels of gp160, gp41, and gp120. The levels of gp160 and gp41 were higher than that of gp120 in this case, as well.

The impact on viral entry of alanine mutation in the JRFL Env sequence was varied. Only two mutants, L669A and I682A,

showed enhanced levels in viral entry and increased Env expression levels. Each of these mutations showed dramatically higher levels of gp160, gp41, and gp120 in both the virus-producing cells and the virus samples.

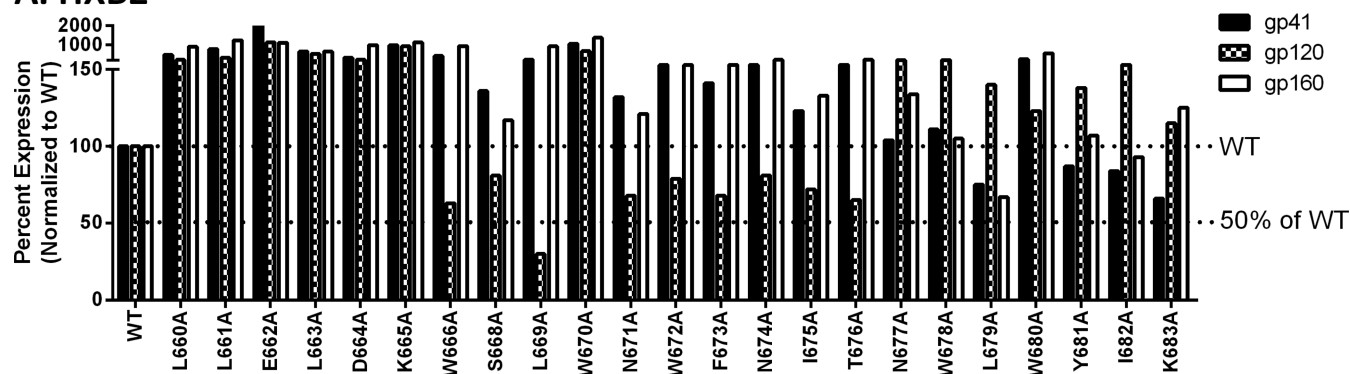
Of the mutations with levels that were decreased to 50% or below the level of WT (K665A, W670A, F673A, T676A, L679A, Y681A, and K683A), many had protein levels near the WT level or higher (W670A, F673A, T676A, L679A, Y681A, and K683A). This indicates a fusion defect. On the other hand, K665A had dramatically lowered levels of gp160 in the producer cell lysate while all levels of gp41 and gp120 both in the producer cell lysate and in the virus sample were elevated above WT levels.

There are also two mutants, N671A and W672A, that had smaller amounts of gp120, while the viral entry levels were approximately 50%. The case of N671 is quite dramatic with undetectable gp120 levels on the virus. Taken together with the results of cell–cell fusion in which these two mutations had an impact on gp120 levels, as well, there is most likely a defect in association between gp41 and gp120.

DISCUSSION

In this study, the effects of alanine substitutions in the HIV gp41 MPER domain were extensively characterized in two different HIV-1 strains, one CCR5-utilizing strain (JRFL) and one CXCR4-utilizing strain (HXB2), by a side-by-side scanning mutation approach. Consistent with a previous report by our group,⁴¹ HXB2 was more stable to alanine substitution in the

A. HXB2



B. JRFL

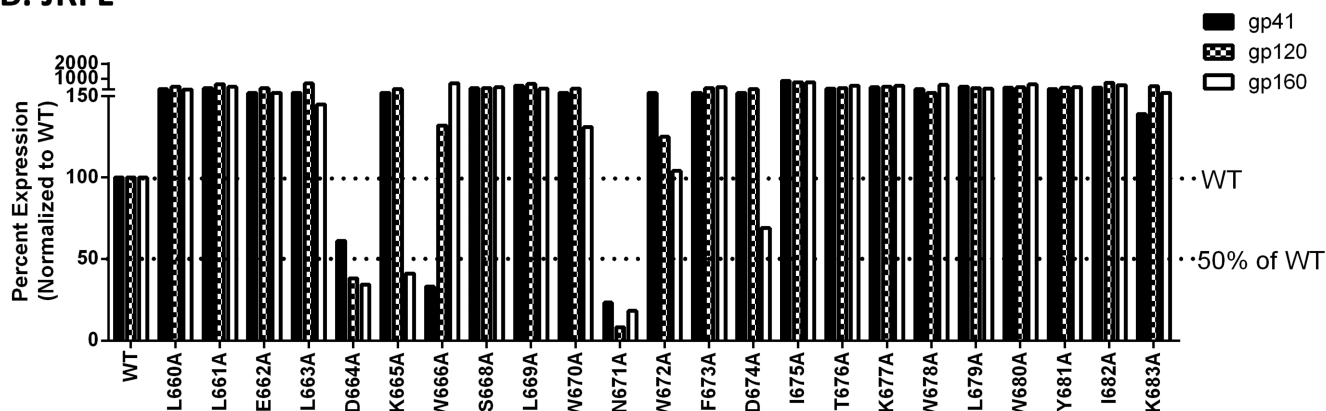


Figure 5. Protein expression level in the lysates of the virus-producing cells. 293T cells were used to produce virus. These cells were lysed, and the protein concentration was quantified by a BCA assay. Subsequent Western blot analysis was performed using Chessie-8 and anti-gp120 antibodies followed by band quantification as described in the legend of Figure 4. Each membrane was reprobed with anti-p24 antibodies, and band intensity was quantified. Each band intensity of gp41, gp160, and gp120 was normalized to the p24 level and then normalized again to the WT level of each protein: (A) protein expression level of HXB2 virus-producing cells and (B) protein expression level of JRFL virus-producing cells.

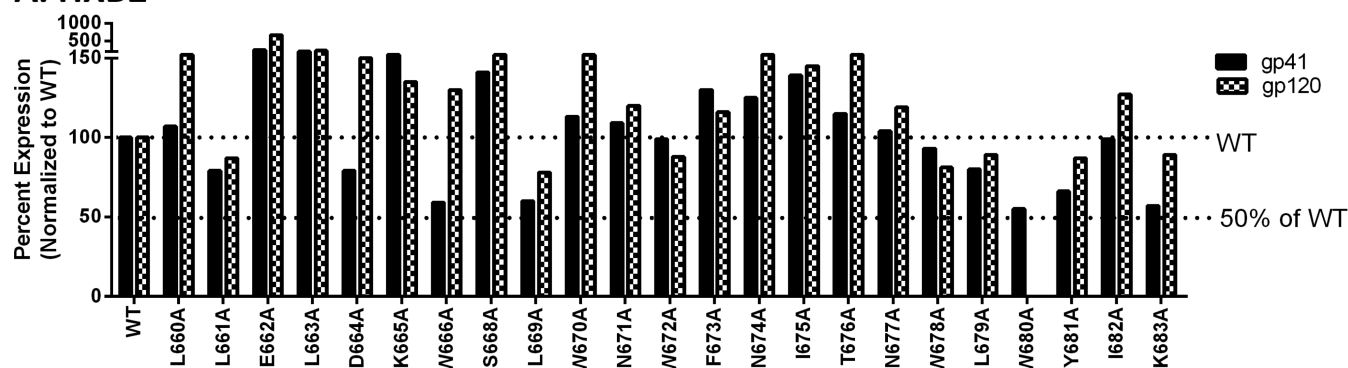
MPER as it had also been shown to be in the C-terminal heptad repeat (CHR) compared to JRFL.

Cell–cell fusion assays have not always correlated with the results from viral entry assays.^{41,54–58} This suggests that the envelope proteins function differently in these two processes. In the case of cell–cell fusion, the envelope is mediating the binding and fusion between two cells of relatively similar size via fusion of the plasma membranes of the envelope-expressing and target cells. The HIV viral particle has been observed to fuse at neutral pH without the need for endosomal internalization.^{59,60} It has also been observed to enter via an endosomal pathway.⁶¹ In the case of fusion at the plasma membrane, as the diameter of mature HIV (approximately 110–128 nm⁶²) is much smaller than the receptor cell, the envelope protein complex is mediating binding and fusion between the more highly curved viral membrane and the larger receptor cell plasma membrane. However, if endocytosis is a productive route of entry, the fusion event occurs between the endosomal membrane and the viral membrane, which more closely resemble each other in size and curvature.⁶¹ Further biophysical and ultrastructural studies of the two processes, cell–cell fusion and viral entry, are warranted to provide insight into the differences in the mechanistic function of the membrane fusion protein complexes. However, the results of the viral entry assays are more relevant for drug and vaccine development as the physiological role of cell–cell fusion in the host has not been conclusively shown.

HXB2 Cell–Cell Fusion. There are several specific residues from each of the strains that warrant further discussion. In HXB2, there is only one residue that stands out as being impacted in cell–cell fusion, D664. Indeed, mutation of this residue to alanine did not significantly impact any of the protein levels. This suggests a critical role in promoting cell–cell fusion for this residue. Many of the mutants that had impacts on viral entry in the case of HXB2 had very little effect on expression, processing, incorporation, or association, which also suggests that the step impacted was membrane fusion. gp160 levels were rarely impacted in the case of HXB2 in lysates from cell–cell fusion or in lysates from virus-producing cells, indicating that expression of Env for strain HXB2 is stable to mutation.

HXB2 Viral Entry. The protein levels measured on virus-producing cells in the case of mutation HXB2 L669A suggest an association defect. The gp120 level is much lower than the gp160 and gp41 levels. However, the levels of gp120 and gp41 on the virus are not dramatically different from one another or greatly reduced. This suggests that in the case of the L669A mutant, shedding of gp120 at the cell surface may be occurring, yet the virus is able to bud with envelope complexes that have similar amounts of gp41 and gp120. In contrast, W680A seems to have both a defect in the incorporation of gp41 into the virion and a defect in gp120–gp41 association. However, the protein levels in the producer cell lysates are at or above the WT level. These differences in incorporation into the virion within a distance of 11 amino acid residues suggest that the envelope complex is sensitive to changes that may be due to

A. HXB2



B. JRFL

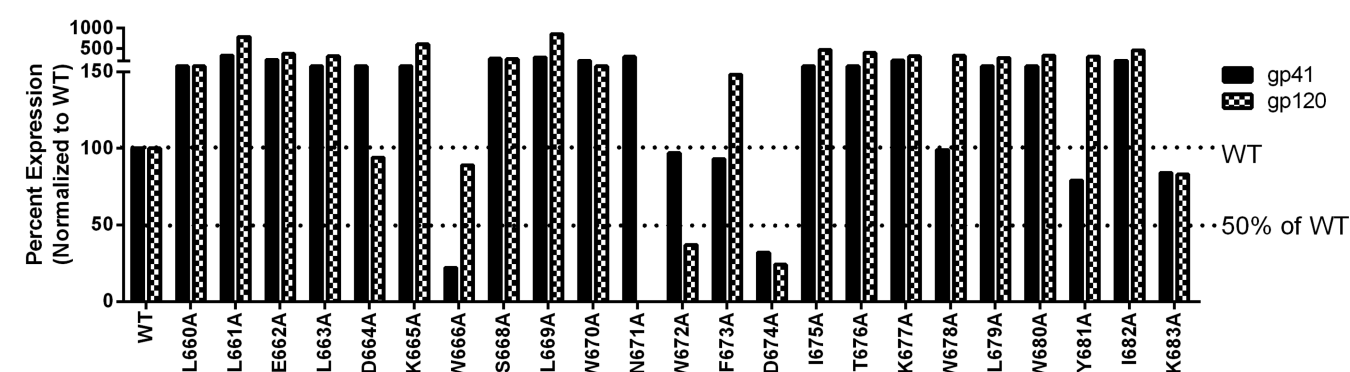


Figure 6. Protein levels on the virus. Concentrated viruses with each mutant Env were lysed followed by Western blot analysis performed as described above: (A) protein level on HXB2 virus and (B) protein level on JRFL virus.

long-range effects upon the global structure of the large multimeric membrane complex.

W670A and N674A were both enhanced in viral entry. In the case of both W670A and N674A, there is a larger amount of gp120 protein in the virus sample than gp41. Levels in the producer cells are high for gp160, gp120, and gp41 in the case of W670A. On the other hand, the level of gp120 is lower than the WT level and lower than gp160 and gp41 levels in the producer cell line for N674A. It is interesting to note that the enhanced level of gp120 as compared to that of gp41 correlates with enhanced viral entry in both mutants.

JRFL Cell–Cell Fusion. In the case of JRFL, a number of mutants with WT or enhanced fusion levels had a smaller amount of gp120 (L660A, K665A, S668A, W678A, L679A, W680A, Y681A, and I682A). This suggests that gp41 can mediate membrane fusion between the plasma membranes of cells expressing envelope and cells expressing the receptors despite a smaller amount of gp120. This could be an artifact of a cell population that has been transfected to express only envelope protein and has no budding virus particles. A gp41–gp120 association defect could result in rapid release of gp120 into the extracellular milieu immediately after cleavage and presentation on the plasma membrane. This would lead to a decreased amount of gp120 that could be detected in the cell lysate. In the case of L663A and N671A, the abolished levels of cell–cell fusion correlated with low levels of gp120, which is to be expected. W666A has an apparent fusogenicity defect as studied in cell–cell fusion as all protein levels were at the wild-type level or higher, yet the level of cell–cell fusion was dramatically decreased.

JRFL Viral Entry. There are many mutations within the C-terminal half of this region of JRFL that have a clear defect in

the fusion step of viral entry, which we can conclude on the basis of functional levels being at or below 50% but protein levels of gp160, gp41, and gp120 at WT or greater levels (W670A, F673A, T676A, L679A, Y681A, and K683A). K665A had a low level of gp160, yet the levels of gp41 and gp120 were greater than those of the wild type. This was the case both in the virus-producing cells and in the protein levels on the virus. Despite the elevated levels of gp41 and gp120, entry levels were diminished. There is a possibility that gp160 in this case is cleaved more efficiently. If this is the case, then there also appears to be a fusogenicity defect. This mutant is likely causing multiple defects. N671A and W6712A also produced anomalous results. Although there seems to be a dramatic effect on gp41–gp120 association, entry levels were around 50%.

In general, the protein levels (gp120 and gp41) in the virus particles in the case of strain JRFL were quite stable; however, mutations often led to defects in entry, suggesting an important role in membrane fusion. There is also the possibility that long-range conformational effects could be caused by mutation that would affect binding of gp120 to the receptors or that the larger global structure of the multisubunit complex could be altered. Ultrastructural studies of this complex at different stages during the entry process are warranted but technically challenging.

Correlation Analysis between HXB2 and JRFL. We performed a correlation analysis between the mutants in HXB2 and JRFL using the data sets for cell–cell fusion and viral entry (GraphPad Prism). The calculated Pearson's r was -0.188 for the cell–cell fusion data set and -0.147 for the viral entry data set. A value of -1 represents perfect negative correlation. In both the cell–cell fusion and viral entry data sets, there was a

relatively small negative correlation between the results for the two strains.

Comparison with Previously Published Alanine Substitutions in the MPER. To the best of our knowledge, this is the first report of an extensive comparison of cell–cell fusion and viral entry using alanine scanning mutagenesis of the HIV MPER for both a CCR5- and a CXCR4-utilizing strain of HIV-1. A summary of previously published results for mutation to alanine in this region is given in Table 3. The alanine

Table 3. Published Results for Alanine Substitutions Performed in the gp41 MPER Region

residue	strain	effect of alanine mutation
L660A	JR2	<30% of WT infectivity ⁶³
L661A	JR2	infectivity similar to that of WT ⁶³
E662A	JR2	infectivity similar to that of WT ⁶³
L663A	JR2	infectivity similar to that of WT ⁶³
D664A	JR2	infectivity similar to that of WT ⁶³
K665A	JR2	infectivity similar to that of WT ⁶³
W666A	JR2	<10% of WT infectivity ⁶³
	HXB2	expression processing, gp120 association, and cell–cell fusion similar to those of WT ³
S668A	JR2 (N668A)	infectivity similar to that of WT ⁶³
L669A	JR2	<30% of WT infectivity ⁶³
W670A	JR2	>30% of WT infectivity ⁶³
	HXB2	expression processing, gp120 association, and cell–cell fusion similar to those of WT ³
N671A	JR2	infectivity similar to that of WT ⁶³
W672A	JR2	<30% of WT infectivity ⁶³
F673A	JR2	infectivity similar to that of WT ⁶³
N674A	JR2	infectivity similar to that of WT ⁶³
I675A	JR2	<30% of WT infectivity ⁶³
T676A	JR2	>30% of WT infectivity ⁶³
N677A	JR2	infectivity similar to that of WT ⁶³
W678A	JR2	>30% of WT infectivity ⁶³
	HXB2, NL4-3	expression processing, gp120 association, and cell–cell fusion similar to those of WT ³
	HXBc2	processing to WT level, but slightly reduced level of association of gp120; cell–cell fusion similar to that of WT ⁶⁴
L679A	JR2	<30% of WT infectivity ⁶³
W680A	JR2	>30% of WT infectivity ⁶³
	HXB2, NL4-3	expression processing, gp120 association, and cell–cell fusion similar to those of WT ³

mutation at L660 in the JR2 strain had a severe defect on virus infectivity;⁶³ however, our results showed only a modest defect because of mutation of this residue to alanine. The mutation of L661 had a WT level in JR2 Env-mediated viral entry,⁶³ whereas this mutation had a modest impact in HXB2 viral entry in our study. Residue E662 had a normal level in viral entry with the JR2 strain, in agreement with our study. L663A was reported to have no impact on viral entry with the JR2 strain,⁶³ whereas in our study, this mutation was impaired in HXB2 viral entry and in JRFL cell–cell fusion. The D664A mutation was reported to have no effect in JR2 viral entry, whereas it showed a severe impact in HXB2 cell–cell fusion and a modest effect in HXB2 and JRFL viral entry in our study. The K665A mutation was reported to have no effect in JR2 viral entry;⁶³ however, it did cause a defect in both HXB2 and JRFL viral entry in our study.

W666A also had the most severe impact on viral infectivity in the JR2 strain;⁶³ however, our results showed only a modest effect on viral entry for either strain. In the case of cell–cell

fusion with the JRFL strain, this was the only residue with a severe defect. The W666A mutant was previously reported for the HXB2 strain³ and resulted in expression, processing, gp120 association, and cell–cell fusion levels similar to those of WT, in agreement with our results.

The alanine mutation of residue 668 (S in HXB2 and JRFL and N in JR2) showed no effect on JR2 viral entry,⁶³ which is consistent with what we observed in both HXB2 and JRFL viral entry. L669A of JR2 showed a severe reduction in viral infectivity compared to the infectivity of the WT JR2 strain,⁶³ in agreement with our data for HXB2 viral entry. The W670A mutation in the JR2 strain was reported to have a decreased level of viral entry,⁶³ in agreement with our results for JRFL viral entry.

While the N671A mutation in JRFL in our cell–cell fusion study showed a defect in cleavage, the N671A mutation in the JR2 strain had no impact on viral entry.⁶³ While W672A and I675A mutations caused a severe reduction in viral entry in the JR2 strain,⁶³ we did not observe this severe impact. F673A in the JR2 strain had no impact on viral entry,⁶³ whereas our data showed a modest impact on HXB2 and JRFL viral entry. N674A in the JR2 strain also had no impact on viral entry,⁶³ however, it showed an enhanced viral entry level in HXB2. T676A in the JR2 strain⁶³ showed diminished activity in viral entry, in agreement with our study for both HXB2 and JRFL. N677A in the JR2 strain had no impact on viral entry,⁶³ whereas our alanine mutant in HXB2 at this residue had a modest defect in viral entry. There is a report showing a slightly reduced level of association of gp120 with gp41 of the HXBc2 strain⁶⁴ for the W678A mutation, which we saw only in the case of JRFL cell–cell fusion. Our data showed that the L679A mutation in HXB2 produced a severe defect in viral entry in agreement with the previously reported results for JR2 Env-mediated viral entry.⁶³ The W680A mutation had a severe defect in association of gp120 with gp41 in HXB2 viral entry in our study, whereas it was reported that it had no impact on expression, processing, or gp120 association in HXB2 Env-mediated cell–cell fusion, in agreement with our study.³

Structural Implications. Molecular models of the MPER trimer structure are shown in Figure 7. Because there is no MPER structure available until residue K683 as well as no structure of the full length gp41 protein in the 6HB formation, we were not able to model the potential interaction of the MPER with the fusion peptide region. To improve our understanding of the effects of mutation in the MPER, we took the membrane-associated MPER trimer model³⁸ and compared the locations of residues that are affected by alanine mutations.

Mutations that affect viral entry were located in the proximity of the viral membrane. Interestingly, the membrane proximal residues, including L679, W680, Y681, and K683A, in HXB2 were severely affected in viral entry by alanine mutations, whereas mutations of these residues either enhance or have only modest effect in the JRFL strain. This could suggest that mutations affect the orientation of aromatic residues that can then affect the stability of the whole gp41 structure, leading to defects in fusogenicity. This is plausible because these residues are also known to play an important role in fusion pore expansion⁴ and changes in orientation may cause distinct defects in the process.

Another important observation is that mutations that affected membrane fusion were mostly on the side of the MPER oriented toward the N-terminal heptad repeat/fusion peptide in

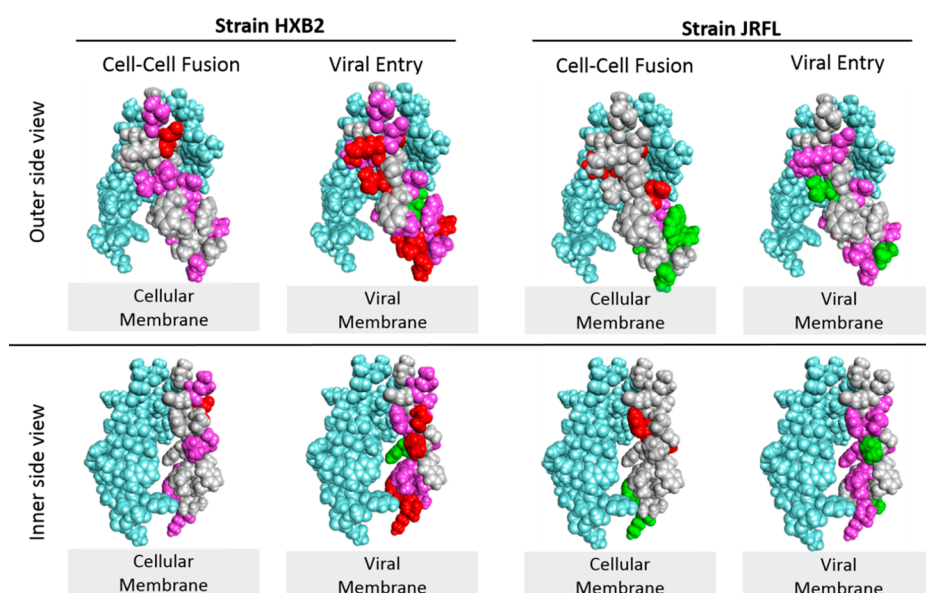


Figure 7. Molecular models highlighting the functionality of mutations in the HIV gp41 MPER. A membrane-associated MPER trimer structure was used to diagram the residues whose functions are either diminished or enhanced upon mutation to alanine.³⁸ For the sake of simplicity, mutations are indicated only on one of the monomers (light gray) and the other two monomers making up the trimer structure are colored light blue. The top panel is a view of the outer side of the MPER. The bottom panel is a view that is rotated to display the inner side of the MPER. Amino acid residues without highlighting (light gray) have levels that are 80–120% of the WT level. Those colored pink have levels diminished to 20–50% of the WT level. Those colored red have levels diminished to <20% of the WT level. The residues colored green have levels increased above 120% of the WT level. The structure was rendered with Discovery Studio Visualizer 4.0 based upon the coordinates from Protein Data Bank 2LP7.

the postfusion structure.^{30,32,33,65–69} This suggests that the MPER interacts with fusion peptide and/or other NHR domain sequences and mutations on the MPER may interfere with the interaction between them in the process of either folding or unfolding during the steps in the fusion mechanism.

It is very interesting as well that we observed different effects of mutations on the two HIV-1 strains despite the high degree of sequence conservation between them (Figure 1). There are only two amino acid residues that are different between these two strains in the MPER. HIV gp41 has a distinct sensitivity to mutation between different strains that seems to be sequence-independent but nonetheless can be affected on a functional level. This suggests the possibility that there are direct interactions or long-range structural changes affecting the MPER that are caused by regions that are not conserved within the gp41 sequence (e.g., fusion peptide).

It is also intriguing that there are significant differences in the effects of alanine mutagenesis between cell–cell fusion and cell-free viral entry. This type of difference between modes of virus transmission has been reported not only by us but also by other groups. Many studies presented loss of susceptibility to entry inhibitors and neutralizing antibodies (nAbs) targeting HIV-1 Env in transmission of virus between cells, while these remained effective in cell-free virus infection. For example, nAb2 4E10 and 2F5 (targeting the MPER), 17b (targeting a CD4-induced epitope), and b12 (targeting the CD4 binding site) were not always observed as effective at inhibiting Env-mediated cell–cell transmission.^{54–57} A recent investigation also revealed that antibodies targeting the CD4 binding site such as CD4-IgG2, VRC01, and b12 lost their inhibitory activity easily only in the case of cell–cell virus transmission while their activity remained during viral entry.⁵⁸ Taken together, these studies along with the report presented here suggest that there are dramatic mechanistic differences between cell–cell fusion and virus cell entry that have implications for

vaccine development. This body of knowledge points to the need to carefully discriminate between targets, especially when considering the design of a prophylactic vaccine versus a therapeutic vaccine. Targeting viral entry will be important in the case of a prophylactic vaccine, while targeting the mechanism of transmission of virus between cells will be important in the case of a potential therapeutic vaccine.

Our comparative mutagenesis study of the MPER suggests that the current discrepancies in the details of the MPER structure reported based upon *in vitro* studies may very well be real and related to mechanistic differences between strains. For example, while one X-ray crystallography study reported an asymmetric dimer of α -helical MPER constructs had utilized prototype B strain HXB2 gp41 sequence,³⁴ another structural study suggesting the MPER portion with a slightly bent helix structure used a subtype A isolate from Cameroon.³⁵ Another structural study of the trimeric MPER showed a symmetrical α -helical conformation with a bend between the 2F5 and 4E10 epitopes and used B/F1 recombinant isolate 01BAB055.³⁸ Furthermore, even with the same HXB2 gp41 MPER, different structures were suggested. For instance, a study that used HXB2 sequence showed an $\sim 90^\circ$ turn of the MPER at N677³⁶ that had not been observed previously.³⁴ On a membrane surface, the HXB2 MPER showed a metastable L-shaped structure,¹⁶ but another study showed the MPER with at least two stable conformations in the lipid bilayer.³⁹

The MPER has been one of the most promising targets in the approach to eliciting neutralizing antibodies because of the broadly neutralizing antibodies 2F5 and 4E10.^{5–14} However, our study suggests that there may be significant differences between virus strains in how localized regions are involved in cell–cell fusion and viral entry. The discrepancies reported for this region from *in vitro* structural studies if considered in the context of the dramatic differences we see between strains using mutagenesis studies in cell culture may well be real differences

implying a structural plasticity in this region important for consideration in vaccine and drug design.

Another critical issue is that exposure of these vulnerable regions during the entry process is limited in time frame. The MPER is not exposed on the native virus particle before interaction with the receptors.²⁸ Interestingly, researchers have suggested that specific single-amino acid changes in gp41 could potentially expose epitopes for neutralization by antibodies.²⁵ If this is indeed possible, our scanning mutagenesis suggests that mutations L660A and E662A from both strains may potentially be useful for manipulating the protein for better exposure of the MPER to raise neutralizing antibodies without altering function.

Finally, the amino acid positions that are unchanged (light gray) can be seen as potential candidates for manipulation to facilitate labeling for highly desired ultrastructural studies. Many of the MPER residues were shown to be stable to alanine mutations. These are potential sites to manipulate with cutting edge labeling that will allow researchers to study the details of gp41 function.

AUTHOR INFORMATION

Corresponding Author

*Address: 109 BRB, 3435 Main St., Buffalo, NY 14214. E-mail: ajacobs2@buffalo.edu. Telephone: (716) 829-2087. Fax: (716) 829-2111.

Funding

This research was supported by the National Institute of Allergy and Infectious Diseases of the National Institutes of Health via Grant R21 AI02796. This work was supported in part by the University of Rochester Center for AIDS Research National Institutes of Health Grant P30AI078498.

Notes

The authors declare no competing financial interest.

ACKNOWLEDGMENTS

The following reagents were obtained through the NIH AIDS Research and Reference Reagent Program, Division of AIDS, National Institute of Allergy and Infectious Diseases, National Institutes of Health: TZM-bl from Dr. John C. Kappes, Dr. Xiaoyun Wu, and Tranzyme Inc.,⁴⁸ pNL4-3.HSAR-E- from Dr. Nathaniel Landau,⁴⁷ pHBX2-env from Dr. Kathleen Page and Dr. Dan Littman,⁴³ pRev-1 from Dr. Marie-Louise Hammarskjöld and Dr. David Rekosh,⁴⁵ pCEP4-Tat from Dr. Lung-Ji Chang,⁴⁶ Chessie-8 from Dr. George Lewis,⁵² and HIV-1 p24 hybridoma (183-H12-5C) from Dr. Bruce Chesebro.⁵³ We thank Dr. James M. Binley (Torrey Pines Institute for Molecular Studies) for the gift of pCAGGS JRFL WT 160.

REFERENCES

- (1) Caffrey, M. (2011) HIV envelope: Challenges and opportunities for development of entry inhibitors. *Trends Microbiol.* 19, 191–197.
- (2) Muster, T., Steindl, F., Purtscher, M., Trkola, A., Klima, A., Himmler, G., Rucker, F., and Katinger, H. (1993) A conserved neutralizing epitope on gp41 of human immunodeficiency virus type 1. *J. Virol.* 67, 6642–6647.
- (3) Salzwedel, K., West, J. T., and Hunter, E. (1999) A conserved tryptophan-rich motif in the membrane-proximal region of the human immunodeficiency virus type 1 gp41 ectodomain is important for Env-mediated fusion and virus infectivity. *J. Virol.* 73, 2469–2480.
- (4) Muñoz-Barroso, I., Salzwedel, K., Hunter, E., and Blumenthal, R. (1999) Role of the membrane-proximal domain in the initial stages of

human immunodeficiency virus type 1 envelope glycoprotein-mediated membrane fusion. *J. Virol.* 73, 6089–6092.

- (5) Montero, M., van Houten, N. E., Wang, X., and Scott, J. K. (2008) The membrane-proximal external region of the human immunodeficiency virus type 1 envelope: Dominant site of antibody neutralization and target for vaccine design. *Microbiol. Mol. Biol. Rev.* 72, 54–84.

- (6) Karlsson Hedestam, G. B., Fouchier, R. A., Phogat, S., Burton, D. R., Sodroski, J., and Wyatt, R. T. (2008) The challenges of eliciting neutralizing antibodies to HIV-1 and to influenza virus. *Nat. Rev. Microbiol.* 6, 143–155.

- (7) Burton, D. R., Desrosiers, R. C., Doms, R. W., Koff, W. C., Kwong, P. D., Moore, J. P., Nabel, G. J., Sodroski, J., Wilson, I. A., and Wyatt, R. T. (2004) HIV vaccine design and the neutralizing antibody problem. *Nat. Immunol.* 5, 233–236.

- (8) Nelson, J. D., Brunel, F. M., Jensen, R., Crooks, E. T., Cardoso, R. M., Wang, M., Hessel, A., Wilson, I. A., Binley, J. M., Dawson, P. E., Burton, D. R., and Zwick, M. B. (2007) An affinity-enhanced neutralizing antibody against the membrane-proximal external region of human immunodeficiency virus type 1 gp41 recognizes an epitope between those of 2F5 and 4E10. *J. Virol.* 81, 4033–4043.

- (9) Binley, J. M., Wrinn, T., Korber, B., Zwick, M. B., Wang, M., Chappey, C., Stiegler, G., Kunert, R., Zolla-Pazner, S., Katinger, H., Petropoulos, C. J., and Burton, D. R. (2004) Comprehensive cross-clade neutralization analysis of a panel of anti-human immunodeficiency virus type 1 monoclonal antibodies. *J. Virol.* 78, 13232–13252.

- (10) Mascola, J. R., Lewis, M. G., Stiegler, G., Harris, D., VanCott, T. C., Hayes, D., Louder, M. K., Brown, C. R., Sapan, C. V., Frankel, S. S., Lu, Y., Robb, M. L., Katinger, H., and Bix, D. L. (1999) Protection of macaques against pathogenic simian/human immunodeficiency virus 89.6PD by passive transfer of neutralizing antibodies. *J. Virol.* 73, 4009–4018.

- (11) Mascola, J. R., Stiegler, G., VanCott, T. C., Katinger, H., Carpenter, C. B., Hanson, C. E., Beary, H., Hayes, D., Frankel, S. S., Bix, D. L., and Lewis, M. G. (2000) Protection of macaques against vaginal transmission of a pathogenic HIV-1/SIV chimeric virus by passive infusion of neutralizing antibodies. *Nat. Med.* 6, 207–210.

- (12) Huang, J., Ofek, G., Laub, L., Louder, M. K., Doria-Rose, N. A., Longo, N. S., Imamichi, H., Bailer, R. T., Chakrabarti, B., Sharma, S. K., Alam, S. M., Wang, T., Yang, Y., Zhang, B., Migueles, S. A., Wyatt, R., Haynes, B. F., Kwong, P. D., Mascola, J. R., and Connors, M. (2012) Broad and potent neutralization of HIV-1 by a gp41-specific human antibody. *Nature* 491, 406–412.

- (13) Zwick, M. B., Labrijn, A. F., Wang, M., Spenlehauer, C., Saphire, E. O., Binley, J. M., Moore, J. P., Stiegler, G., Katinger, H., Burton, D. R., and Parren, P. W. H. I. (2001) Broadly neutralizing antibodies targeted to the membrane-proximal external region of human immunodeficiency virus type 1 glycoprotein gp41. *J. Virol.* 75, 10892–10905.

- (14) Stiegler, G., Kunert, R., Purtscher, M., Wolbank, S., Voglauer, R., Steindl, F., and Katinger, H. (2001) A potent cross-clade neutralizing human monoclonal antibody against a novel epitope on gp41 of human immunodeficiency virus type 1. *AIDS Res. Hum. Retroviruses* 17, 1757–1765.

- (15) Song, L., Sun, Z. Y., Coleman, K. E., Zwick, M. B., Gach, J. S., Wang, J. H., Reinherz, E. L., Wagner, G., and Kim, M. (2009) Broadly neutralizing anti-HIV-1 antibodies disrupt a hinge-related function of gp41 at the membrane interface. *Proc. Natl. Acad. Sci. U.S.A.* 106, 9057–9062.

- (16) Sun, Z. Y., Oh, K. J., Kim, M., Yu, J., Brusic, V., Song, L., Qiao, Z., Wang, J. H., Wagner, G., and Reinherz, E. L. (2008) HIV-1 broadly neutralizing antibody extracts its epitope from a kinked gp41 ectodomain region on the viral membrane. *Immunity* 28, 52–63.

- (17) Wild, C., Greenwell, T., and Matthews, T. (1993) A synthetic peptide from HIV-1 gp41 is a potent inhibitor of virus-mediated cell fusion. *AIDS Res. Hum. Retroviruses* 9, 1051–1053.

- (18) Wild, C. T., Shugars, D. C., Greenwell, T. K., McDaniel, C. B., and Matthews, T. J. (1994) Peptides corresponding to a predictive α -helical domain of human immunodeficiency virus type 1 gp41 are

potent inhibitors of virus infection. *Proc. Natl. Acad. Sci. U.S.A.* 91, 9770–9774.

(19) Furuta, R. A., Wild, C. T., Weng, Y., and Weiss, C. D. (1998) Capture of an early fusion-active conformation of HIV-1 gp41. *Nat. Struct. Biol.* 5, 276–279.

(20) Kim, M., Song, L., Moon, J., Sun, Z. Y., Bershteyn, A., Hanson, M., Cain, D., Goka, S., Kelsoe, G., Wagner, G., Irvine, D., and Reinherz, E. L. (2013) Immunogenicity of membrane-bound HIV-1 gp41 membrane-proximal external region (MPER) segments is dominated by residue accessibility and modulated by stereochemistry. *J. Biol. Chem.* 288, 31888–31901.

(21) Zhou, T., Zhu, J., Yang, Y., Gorman, J., Ofek, G., Srivatsan, S., Druz, A., Lees, C. R., Lu, G., Soto, C., Stuckey, J., Burton, D. R., Koff, W. C., Connors, M., and Kwon, P. D. (2014) Transplanting supersites of HIV-1 vulnerability. *PLoS One* 9, e99881.

(22) Morris, L., Chen, X., Alam, M., Tomaras, G., Zhang, R., Marshall, D. J., Chen, B., Parks, R., Foulger, A., Jaeger, F., Donathan, M., Bilska, M., Gray, E. S., Abdool Karim, S. S., Kepler, T. B., Whitesides, J., Montefiori, D., Moody, M. A., Liao, H. X., and Haynes, B. F. (2011) Isolation of a human anti-HIV gp41 membrane proximal region neutralizing antibody by antigen-specific single B cell sorting. *PLoS One* 6, e23532.

(23) Kim, M., Sun, Z. Y., Rand, K. D., Shi, X., Song, L., Cheng, Y., Fahmy, A. F., Majumdar, S., Ofek, G., Yang, Y., Kwong, P. D., Wang, J. H., Engen, J. R., Wagner, G., and Reinherz, E. L. (2011) Antibody mechanics on a membrane-bound HIV segment essential for GP41-targeted viral neutralization. *Nat. Struct. Mol. Biol.* 18, 1235–1243.

(24) Ofek, G., Guenaga, F. J., Schief, W. R., Skinner, J., Baker, D., Wyatt, R., and Kwong, P. D. (2010) Elicitation of structure-specific antibodies by epitope scaffolds. *Proc. Natl. Acad. Sci. U.S.A.* 107, 17880–17887.

(25) Blish, C. A., Nguyen, M. A., and Overbaugh, J. (2008) Enhancing exposure of HIV-1 neutralization epitopes through mutations in gp41. *PLoS Med.* 5, e9.

(26) Chakrabarti, B. K., Walker, L. M., Guenaga, J. F., Ghobbeh, A., Poignard, P., Burton, D. R., and Wyatt, R. T. (2011) Direct antibody access to the HIV-1 membrane-proximal external region positively correlates with neutralization sensitivity. *J. Virol.* 85, 8217–8226.

(27) Ofek, G., Tang, M., Sambor, A., Katinger, H., Mascola, J. R., Wyatt, R., and Kwong, P. D. (2004) Structure and mechanistic analysis of the anti-human immunodeficiency virus type 1 antibody 2F5 in complex with its gp41 epitope. *J. Virol.* 78, 10724–10737.

(28) Dimitrov, A. S., Jacobs, A., Finnegan, C. M., Stiegler, G., Katinger, H., and Blumenthal, R. (2007) Exposure of the membrane-proximal external region of HIV-1 gp41 in the course of HIV-1 envelope glycoprotein-mediated fusion. *Biochemistry* 46, 1398–1401.

(29) Frey, G., Peng, H., Rits-Volloch, S., Morelli, M., Cheng, Y., and Chen, B. (2008) A fusion-intermediate state of HIV-1 gp41 targeted by broadly neutralizing antibodies. *Proc. Natl. Acad. Sci. U.S.A.* 105, 3739–3744.

(30) Tan, K., Liu, J., Wang, J., Shen, S., and Lu, M. (1997) Atomic structure of a thermostable subdomain of HIV-1 gp41. *Proc. Natl. Acad. Sci. U.S.A.* 94, 12303–12308.

(31) Malashkevich, V. N., Chan, D. C., Chutkowski, C. T., and Kim, P. S. (1998) Crystal structure of the simian immunodeficiency virus (SIV) gp41 core: Conserved helical interactions underlie the broad inhibitory activity of gp41 peptides. *Proc. Natl. Acad. Sci. U.S.A.* 95, 9134–9139.

(32) Weissenhorn, W., Dessen, A., Harrison, S. C., Skehel, J. J., and Wiley, D. C. (1997) Atomic structure of the ectodomain from HIV-1 gp41. *Nature* 387, 426–430.

(33) Chan, D. C., Fass, D., Berger, J. M., and Kim, P. S. (1997) Core structure of gp41 from the HIV envelope glycoprotein. *Cell* 89, 263–273.

(34) Liu, J., Deng, Y., Li, Q., Dey, A. K., Moore, J. P., and Lu, M. (2010) Role of a putative gp41 dimerization domain in human immunodeficiency virus type 1 membrane fusion. *J. Virol.* 84, 201–209.

(35) Shi, W., Bohon, J., Han, D. P., Habte, H., Qin, Y., Cho, M. W., and Chance, M. R. (2010) Structural characterization of HIV gp41 with the membrane-proximal external region. *J. Biol. Chem.* 285, 24290–24298.

(36) Buzon, V., Natrajan, G., Schibli, D., Campelo, F., Kozlov, M. M., and Weissenhorn, W. (2010) Crystal structure of HIV-1 gp41 including both fusion peptide and membrane proximal external regions. *PLoS Pathog.* 6, e1000880.

(37) Alam, S. M., Morelli, M., Dennison, S. M., Liao, H. X., Zhang, R., Xia, S. M., Rits-Volloch, S., Sun, L., Harrison, S. C., Haynes, B. F., and Chen, B. (2009) Role of HIV membrane in neutralization by two broadly neutralizing antibodies. *Proc. Natl. Acad. Sci. U.S.A.* 106, 20234–20239.

(38) Reardon, P. N., Sage, H., Dennison, S. M., Martin, J. W., Donald, B. R., Alam, S. M., Haynes, B. F., and Spicer, L. D. (2014) Structure of an HIV-1-neutralizing antibody target, the lipid-bound gp41 envelope membrane proximal region trimer. *Proc. Natl. Acad. Sci. U.S.A.* 111, 1391–1396.

(39) Kyrychenko, A., Freitas, J. A., He, J., Tobias, D. J., Wimley, W. C., and Ladokhin, A. S. (2014) Structural plasticity in the topology of the membrane-interacting domain of HIV-1 gp41. *Biophys. J.* 106, 610–620.

(40) Jacobs, A., Sen, J., Rong, L., and Caffrey, M. (2005) Alanine scanning mutants of the HIV gp41 loop. *J. Biol. Chem.* 280, 27284–27288.

(41) Diaz-Aguilar, B., DeWispelaere, K., Yi, H. A., and Jacobs, A. (2013) Significant differences in cell–cell fusion and viral entry between strains revealed by scanning mutagenesis of the C-heptad repeat of HIV gp41. *Biochemistry* 52, 3552–3563.

(42) Sen, J., Yan, T., Wang, J., Rong, L., Tao, L., and Caffrey, M. (2010) Alanine scanning mutagenesis of HIV-1 gp41 heptad repeat 1: Insight into the gp120-gp41 interaction. *Biochemistry* 49, S057–S065.

(43) Page, K. A., Landau, N. R., and Littman, D. R. (1990) Construction and use of a human immunodeficiency virus vector for analysis of virus infectivity. *J. Virol.* 64, S270–S276.

(44) Schulke, N., Vesanen, M. S., Sanders, R. W., Zhu, P., Lu, M., Anselma, D. J., Villa, A. R., Parren, P. W., Binley, J. M., Roux, K. H., Maddon, P. J., Moore, J. P., and Olson, W. C. (2002) Oligomeric and conformational properties of a proteolytically mature, disulfide-stabilized human immunodeficiency virus type 1 gp140 envelope glycoprotein. *J. Virol.* 76, 7760–7776.

(45) Lewis, N., Williams, J., Rekosh, D., and Hammarskjöld, M. L. (1990) Identification of a cis-acting element in human immunodeficiency virus type 2 (HIV-2) that is responsive to the HIV-1 rev and human T-cell leukemia virus types I and II rex proteins. *J. Virol.* 64, 1690–1697.

(46) Chang, L. J., Urlacher, V., Iwakuma, T., Cui, Y., and Zucali, J. (1999) Efficacy and safety analyses of a recombinant human immunodeficiency virus type 1 derived vector system. *Gene Ther.* 6, 715–728.

(47) He, J., Choe, S., Walker, R., Di Marzio, P., Morgan, D. O., and Landau, N. R. (1995) Human immunodeficiency virus type 1 viral protein R (Vpr) arrests cells in the G2 phase of the cell cycle by inhibiting p34cdc2 activity. *J. Virol.* 69, 6705–6711.

(48) Platt, E. J., Wehrly, K., Kuhmann, S. E., Chesebro, B., and Kabat, D. (1998) Effects of CCR5 and CD4 cell surface concentrations on infections by macrophagetropic isolates of human immunodeficiency virus type 1. *J. Virol.* 72, 2855–2864.

(49) Ehrhardt, C., Schmolke, M., Matzke, A., Knoblauch, A., Will, C., Wixler, V., and Ludwig, S. (2006) Polyethylenimine, a cost-effective transfection reagent. *Signal Transduction* 6, 179–184.

(50) Yi, H. A., Diaz-Aguilar, B., Bridon, D., Quraishi, O., and Jacobs, A. (2011) Permanent inhibition of viral entry by covalent entrapment of HIV gp41 on the virus surface. *Biochemistry* 50, 6966–6972.

(51) O'Doherty, U., Swiggard, W. J., and Malim, M. H. (2000) Human immunodeficiency virus type 1 spinoculation enhances infection through virus binding. *J. Virol.* 74, 10074–10080.

(52) Abacioglu, Y. H., Fouts, T. R., Laman, J. D., Claassen, E., Pincus, S. H., Moore, J. P., Roby, C. A., Kamin-Lewis, R., and Lewis, G. K.

(1994) Epitope mapping and topology of baculovirus-expressed HIV-1 gp160 determined with a panel of murine monoclonal antibodies. *AIDS Res. Hum. Retroviruses* 10, 371–381.

(53) Chesebro, B., Wehrly, K., Nishio, J., and Perryman, S. (1992) Macrophage-tropic human immunodeficiency virus isolates from different patients exhibit unusual V3 envelope sequence homogeneity in comparison with T-cell-tropic isolates: Definition of critical amino acids involved in cell tropism. *J. Virol.* 66, 6547–6554.

(54) Yee, M., Konopka, K., Balzarini, J., and Duzgunes, N. (2011) Inhibition of HIV-1 Env-mediated cell-cell fusion by lectins, peptide T-20, and neutralizing antibodies. *Open Virol. J.* 5, 44–51.

(55) Durham, N. D., Yewdall, A. W., Chen, P., Lee, R., Zony, C., Robinson, J. E., and Chen, B. K. (2012) Neutralization resistance of virological synapse-mediated HIV-1 infection is regulated by the gp41 cytoplasmic tail. *J. Virol.* 86, 7484–7495.

(56) McCoy, L., Groppelli, E., Blanchetot, C., de Haard, H., Verrips, T., Rutten, L., Weiss, R., and Jolly, C. (2014) Neutralisation of HIV-1 cell-cell spread by human and llama antibodies. *Retrovirology* 11, 83.

(57) Beck, Z., Brown, B. K., Matyas, G. R., Polonis, V. R., Rao, M., and Alving, C. R. (2011) Infection of human peripheral blood mononuclear cells by erythrocyte-bound HIV-1: Effects of antibodies and complement. *Virology* 412, 441–447.

(58) Abela, I., Berlinger, L., Schanz, M., Reynell, L., Gunthard, H., Rusert, P., and Trkola, A. (2012) Cell-cell transmission enables HIV-1 to evade inhibition by potent CD4bs directed antibodies. *PLoS Pathog.* 8, e1002634.

(59) Stein, B. S., Gowda, S. D., Lifson, J. D., Penhallow, R. C., Bensch, K. G., and Engleman, E. G. (1987) pH-independent HIV entry into CD4-positive T cells via virus envelope fusion to the plasma membrane. *Cell* 49, 659–668.

(60) McClure, M. O., Marsh, M., and Weiss, R. A. (1988) Human immunodeficiency virus infection of CD4-bearing cells occurs by a pH-independent mechanism. *EMBO J.* 7, 513–518.

(61) Miyauchi, K., Kim, Y., Latinovic, O., Morozov, V., and Melikyan, G. B. (2009) HIV enters cells via endocytosis and dynamin-dependent fusion with endosomes. *Cell* 137, 433–444.

(62) Gentile, M., Adrian, T., Scheidler, A., Ewald, M., Dianzani, F., Pauli, G., and Gelderblom, H. R. (1994) Determination of the size of HIV using adenovirus type 2 as an internal length marker. *J. Virol. Methods* 48, 43–52.

(63) Zwick, M. B., Jensen, R., Church, S., Wang, M., Stiegler, G., Kunert, R., Katinger, H., and Burton, D. R. (2005) Anti-human immunodeficiency virus type 1 (HIV-1) antibodies 2F5 and 4E10 require surprisingly few crucial residues in the membrane-proximal external region of glycoprotein gp41 to neutralize HIV-1. *J. Virol.* 79, 1252–1261.

(64) Cao, J., Bergeron, L., Helseth, E., Thali, M., Repke, H., and Sodroski, J. (1993) Effects of amino acid changes in the extracellular domain of the human immunodeficiency virus type 1 gp41 envelope glycoprotein. *J. Virol.* 67, 2747–2755.

(65) Lu, M., Blacklow, S. C., and Kim, P. S. (1995) A trimeric structural domain of the HIV-1 transmembrane glycoprotein. *Nat. Struct. Biol.* 2, 1075–1082.

(66) Caffrey, M., Cai, M., Kaufman, J., Stahl, S. J., Wingfield, P. T., Covell, D. G., Gronenborn, A. M., and Clore, G. M. (1998) Three-dimensional solution structure of the 44 kDa ectodomain of SIV gp41. *EMBO J.* 17, 4572–4584.

(67) Jacobs, A., Simon, C., and Caffrey, M. (2006) Thermostability of the HIV gp41 wild-type and loop mutations. *Protein Pept. Lett.* 13, 477–480.

(68) Krell, T., Greco, F., Engel, O., Dubayle, J., Dubayle, J., Kennel, A., Charlotiaux, B., Brasseur, R., Chevalier, M., Sodoyer, R., and El Habib, R. (2004) HIV-1 gp41 and gp160 are hyperthermostable proteins in a mesophilic environment. Characterization of gp41 mutants. *Eur. J. Biochem.* 271, 1566–1579.

(69) Caffrey, M. (2001) Model for the structure of the HIV gp41 ectodomain: Insight into the intermolecular interactions of the gp41 loop. *Biochim. Biophys. Acta* 1536, 116–122.